Mon. Not. R. Astron. Soc. **351,** 186–192 (2004) doi:10.1111/j.1365-2966.2004.07768.x

Radio detections of the neutron star X-ray binaries 4U 1820 − 30 and Ser X-1 in soft X-ray states

S. Migliari,[1⋆] R. P. Fender,[1⋆] M. Rupen,[2] S. Wachter,[3] P. G. Jonker,[4] J. Homan[5] and M. van der Klis[1]

[1]*Astronomical Institute 'Anton Pannekoek', University of Amsterdam, and Centre for High Energy Astrophysics, Kruislaan 403, 1098 SJ, Amsterdam, the Netherlands*
[2]*National Radio Astronomy Observatory, Socorro, NM 87801, USA*
[3]*SIRTF Science Center, California Institute of Technology, MS 220-6, Pasadena, CA 91125, USA*
[4]*Institute of Astronomy, Madingley Road, Cambridge CB3 0HA*
[5]*MIT Center for Space Research, 77 Massachusetts Avenue, Cambridge, MA 02139, USA*

Accepted 2004 February 23. Received 2004 February 23; in original form 2003 November 24

ABSTRACT

We present the analysis of simultaneous X-ray (*RXTE*) and radio (VLA) observations of two atoll-type neutron star X-ray binaries: 4U 1820 − 30 and Ser X-1. Both sources were steadily in the soft ('banana') X-ray state during the observations. We have detected the radio counterpart of 4U 1820 − 30 at 4.86 and 8.46 GHz at a flux density of ∼0.1 mJy. This radio source is positionally coincident with the radio pulsar PSR 1820 − 30A. However, the radio emission of the pulsar falls rapidly with frequency ($\propto \nu^{-3}$), and we argue that the radio emission of the X-ray binary is dominant above ∼2 GHz. Supporting this interpretation, comparison with previous observations reveals variability at the higher radio frequencies that is likely to be due to the X-ray binary. We have detected for the first time the radio counterpart of Ser X-1 at 8.46 GHz, also at a flux density of ∼0.1 mJy. The position of the radio counterpart has allowed us to identify its optical counterpart unambiguously. We briefly discuss similarities and differences between the disc–jet coupling in neutron star and black hole X-ray binaries. In particular, we draw attention to the fact that, contrary to other states, neutron star X-ray binaries seem to be more radio-loud than persistent black hole candidates when the emission is 'quenched' in the soft state.

Key words: binaries: close – stars: individual: 4U 1820 − 30 – stars: individual: Ser X-1 – stars: neutron – ISM: jets and outflows – radio continuum: stars.

1 INTRODUCTION

Many works suggest that the radio emission in X-ray binaries, even when no spatial structure is resolved, originates in jet-like outflows (Hjellming & Han 1995; Falcke & Biermann 1996; Dhawan, Mirabel & Rodriguez 2000; Fomalont, Geldzahler & Bradshaw 2001; Fender 2004). A X-ray/radio correlation is therefore usually interpreted as a disc–jet coupling in the systems. In black hole candidate (BHC) X-ray binaries a connection between radio emission and X-ray emission is already clear. Studies of BHCs in the low/hard state have shown a strong correlation between X-ray and radio fluxes over more than three orders of magnitude in accretion rate (Hannikainen et al. 1998; Corbel et al. 2000, 2003; Gallo, Fender & Pooley 2003). For X-ray luminosities greater than a few per cent Eddington, where the X-ray spectra soften dramatically, the radio emission seems to be 'quenched' (Fender et al. 1999; Corbel et al. 2001; Gallo et al. 2003).

Low magnetic field neutron star (NS) X-ray binaries have been classified, based on X-ray spectral and timing properties, in two distinct classes, the names of which recall the shape that they trace in the colour–colour diagram (CD): Z-type and atoll-type (Hasinger & van der Klis 1989). The position of the source in the CD defines its X-ray state. In atoll sources the hardest X-ray state is called the 'island' state and the softest the 'banana' state [see Hasinger & van der Klis (1989) for details]. Atoll-type X-ray binaries in the hard state share many X-ray timing and spectral properties with BHCs in the low/hard state (e.g. van der Klis 1994). However, our understanding of the relation between radio activity and X-ray state in these NS sources remains sketchy. This is mainly due to the fact that their radio luminosities are significantly less than in BHs (Fender & Hendry 2000), resulting in a rather small number of atoll sources with identified radio counterparts (Hjellming & Han 1995; Berendsen et al. 2000). Recently, Migliari et al. (2003) found the first evidence for

⋆E-mail: migliari@science.uva.nl (SM); rpf@science.uva.nl (RPF)

disc–jet coupling in an atoll source, analysing simultaneous X-ray and radio observations of the NS X-ray binary 4U 1728 − 34, when the source was in the hard (i.e. mainly island) state. We found positive ranking correlations between the radio flux density and X-ray flux and between the radio flux density and X-ray timing features. We also confirmed quantitatively that in the hard state black hole binaries are ∼30 times more 'radio loud' than atoll-type NSs at a similar Eddington fraction (see also Fender & Kuulkers 2001).

In this paper we analyse simultaneous X-ray and radio observations of two atoll-type NS sources in the X-ray soft (i.e. middle–upper banana) state: 4U 1820 − 30 and Ser X-1 (4U 1837+04).

1.1 4U 1820 − 30

4U 1820 − 30 is a low-mass X-ray binary located in the globular cluster NGC 6624 (Giacconi et al. 1974). A distance of 7.6 ± 0.4 kpc (Heasley et al. 2000) has been derived from optical observations. Grindlay et al. (1976) discovered thermonuclear X-ray bursts in the source, indicating an NS as a compact object. From X-ray burst properties a distance of ∼6.6 kpc can be derived (Vacca, Lewin & van Paradijs 1986; see Kuulkers et al. 2003). Smale, Zhang & White (1997) reported the discovery of kHz quasi-periodic oscillations (QPOs) in 4U 1820 − 30. A correlation between the frequency of the kHz QPOs and the position in the CD was found by Bloser et al. (2000). In particular, in 4U 1820 − 30 the kHz QPOs seem to be present while the source is in the lower banana state and absent when in the upper banana state. The broad-band 2–50 keV spectrum of the source is well fitted with a typical model for atoll sources in the soft state: a blackbody (or a multitemperature disc blackbody) plus a cut-off power law or with a Comptonization model (e.g. CompTT: Titarchuk 1994) plus a blackbody component (e.g. Bloser et al. 2000). The radio source at the position of 4U 1820 − 30 was detected from observations with the Very Large Array (VLA) at 1.4 GHz by Geldzahler (1983) with a flux density of 2.44 ± 0.37 mJy, and then by Grindlay & Seaquist (1986) at the same frequency with a flux density of 0.49 ± 0.12 mJy. The identification of this radio source as the radio counterpart of the X-ray binary is controversial. Johnston & Kulkarni (1992) first identified the radio source that they found at 1.4 GHz at the position of the X-ray binary as the radio counterpart of 4U 1820 − 30. Later, based on the steepness of the spectrum of the radio source (a non-detection at 8.5 GHz with rms ∼20 μJy; see also Biggs et al. 1994, they (Johnston & Kulkarni 1993) identified the radio source as a pulsar. The radio position of this pulsar, PSR 1820 − 30A (Biggs et al. 1990, 1994; Stappers 1997), is coincident with the optical counterpart of the X-ray binary (Sosin & King 1995), and with the most recent VLA detection at 1.5 and 5 GHz (Fruchter & Goss 2000). These two sources are spatially unresolved. This makes the identification of the real origin of the observed radio emission difficult.

1.2 Ser X-1

Ser X-1 was discovered in X-rays in 1965 (Friedmann, Byram & Chubb 1967). The source shows thermonuclear X-ray bursts, reported for the first time by Swank et al. (1976). Ser X-1 is one of the three NS binary systems in which simultaneous X-ray and optical bursts have been observed (Hackwell et al. 1979). Christian & Swank (1997) derived a distance of ∼8.4 kpc from burst properties. The X-ray energy spectrum of the source is reasonably well fitted with the same model as used for 4U 1820 − 30: a soft component, a blackbody or multicolour disc blackbody, and a Comptonized component (e.g. Oosterbroek et al. 2001). The optical counterpart was first identified as a blue star by Davidsen (1975). Subsequently, it turned out that the optical counterpart was in fact two unresolved stars (Thorstensen, Charles & Bowyer 1980). The two Davidsen stars are called DN (north) and DS (south), and DS (now called MM Ser) is the proposed optical counterpart (Thorstensen et al. 1980). Wachter (1997) found that DS is itself the superposition of two previously unresolved stars, DSw (west) and DSe (east), separated by 1 arcsec. The brightest of the two stars (DSe) was suggested to be the real counterpart of Ser X-1 by Wachter (1997). Hynes et al. (2004) deblended the spectra of DSe and DSw and found further spectral confirmation of Wachter's suggestion. At radio wavelengths Grindlay & Seaquist (1986) reported upper limits of <0.4 mJy at 5 GHz.

2 OBSERVATIONS AND DATA ANALYSIS

We have analysed simultaneous radio and X-ray observations of 4U 1820 − 30 and Ser X-1 performed with the VLA and with the *Rossi X-ray Timing Explorer* (*RXTE*). The dates of the observations are shown in Table 1.

2.1 VLA

We have analysed seven observations of 4U 1820 − 30 (the durations of which range from about 40 min to 2 h) and one observation (of about 5 h) of Ser X-1 with the VLA at 4.86 and 8.46 GHz. During the 4U 1820 − 30 observations the VLA was in B configuration, and during the Ser X-1 observation it was in A configuration. For 4U 1820 − 30 we have used 1331+305 (3C 286) as the flux calibrator and 1820 − 254 (J2000 RA $18^{h}20^{m}57\overset{s}{.}8487$, Dec. $-25°28'12\overset{''}{.}587$) as the phase calibrator. For Ser X-1 we have used both 0137+331 (3C 48) and 1331+305 (3C 286) as flux calibrators, and 1824+107 (J2000 RA $18^{h}24^{m}02\overset{s}{.}8554$, Dec. $-10°44'23\overset{''}{.}772$) as the phase calibrator. Flux densities of the two sources measured at both frequencies are shown in Table 1. Many of the data of 4U 1820 − 30 on MJD 52492 had to be discarded because of bad weather, leading to the larger errors in Table 1. The best-fitting coordinates, from fits in the image plane assuming a Gaussian model, for the radio counterpart of 4U 1820 − 30 are J2000 RA $18^{h}23^{m}40\overset{s}{.}4820 \pm 0\overset{s}{.}0088$, Dec. $-30°21'40\overset{''}{.}12 \pm 0\overset{''}{.}16$, and for the radio counterpart of

Table 1. Modified Julian Day (MJD), 2–10 keV unabsorbed flux ($F_{2-10\,\mathrm{keV}}$) in erg s^{-1} cm^{-2}, and radio flux density at 4.86 GHz ($F_{4.86\,\mathrm{GHz}}$) and at 8.46 GHz ($F_{8.46\,\mathrm{GHz}}$) in mJy for seven VLA observations of 4U 1820 − 30 (five of which were simultaneous with *RXTE*) and for one VLA observation (simultaneous with *RXTE*) of Ser X-1. Error bars are 1σ errors.

MJD	$F_{2-10\,\mathrm{keV}}$ (erg s^{-1} cm^{-2})	$F_{4.86\,\mathrm{GHz}}$ (mJy)	$F_{8.46\,\mathrm{GHz}}$ (mJy)
	4U 1820 − 30		
52480[a]	7.9×10^{-9}	0.16 ± 0.10	0.14 ± 0.04
52482	8.7×10^{-9}	0.13 ± 0.10	0.08 ± 0.04
52484	8.7×10^{-9}	0.15 ± 0.09	0.10 ± 0.04
52487	9.0×10^{-9}	0.17 ± 0.09	0.10 ± 0.04
52489	9.2×10^{-9}	0.08 ± 0.09	0.06 ± 0.05
52492[b,c]	...	0.09 ± 0.16	0.04 ± 0.06
52494[b]	...	-0.07 ± 0.10	0.09 ± 0.04
Averaged	8.7×10^{-9}	0.13 ± 0.04	0.10 ± 0.02
	Ser X-1		
52421	4.4×10^{-9}	0.05 ± 0.04	0.08 ± 0.02

[a]The 2–10 keV unabsorbed flux is the averaged flux of the four RXTE observations performed on MJD 52480; [b]not simultaneous with RXTE; [c]bad weather.

Ser X-1 are J2000 RA $18^{\mathrm{h}}39^{\mathrm{m}}57^{\mathrm{s}}.557 \pm 0^{\mathrm{s}}.010$, Dec. $+05°02'09''.50 \pm 0''.14$. The naturally weighted synthesized beamwidth for the combined data of 4U 1820 − 30 is 3.49×1.46 arcsec^2 in position angle $-1°.2$ at 5 GHz and 1.96×0.80 arcsec^2 in position angle $-2°.2$ at 8 GHz, and for Ser X-1 it is 1.51×0.79 arcsec^2 in position angle $+66°.2$ at 5 GHz and 0.77×0.46 arcsec^2 in position angle $+67°.1$ at 8.3 GHz. There is no evidence for any spatial extension to the radio counterparts of either source. Neither 4U 1820 − 30 nor Ser X-1 shows significant radio variability over the time of monitoring.

2.2 *RXTE*

For the *RXTE* observations we have used data from the Proportional Counter Array (PCA; for spectral and timing analysis) and the High Energy X-ray Timing Experiment (HEXTE; only for spectral analysis). We have used the PCA Standard2 data of the proportional counter unit 2 (PCU2; on in all the observations) to produce the CD of all the *RXTE* observations of 4U 1820 − 30 and Ser X-1 available in the public archive. A soft colour and a hard colour are defined as the count rate ratios 3.5–6 keV/2–3.5 keV and 9.7–16 keV/6–9.7 keV, respectively. We have normalized the colours of 4U 1820 − 30 and Ser X-1 to the colours of the Crab calculated with the closest observation available to each observation analysed. Assuming the steadiness of the Crab energy spectrum, this normalization allows us to compare observations in different epochs minimizing shifts in the CD of instrumental origin. In Fig. 1 we show the mean colours (black dots) of each of the public *RXTE* observations of 4U 1820 − 30 (top panel) and Ser X-1 (bottom panel). The observations marked with open circles are simultaneous with radio (VLA) observations. We have analysed in detail (X-ray spectral and timing analysis) only these simultaneous radio/X-ray observations. The open squares mark the observations in which X-ray bursts are observed in the PCA light curve. In the CD of 4U 1820 − 30 (Fig. 1, top) the open triangle shows the observation in which the so-called 'superburst' was discovered (Strohmayer & Brown 2002).

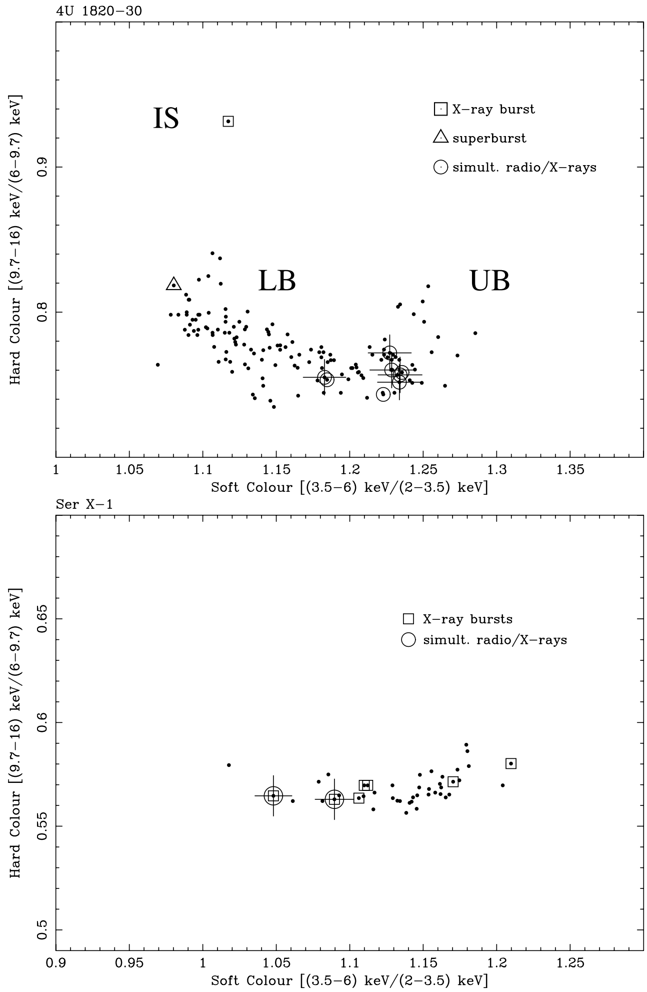

Figure 1. Mean colours (with PCU2 only) of each of all the observations of 4U 1820 − 30 (top panel) and Ser X-1 (bottom panel) in the *RXTE* public archive. The observations marked with open circles are simultaneous with radio (VLA) observations and those marked with open squares are the observations that show X-ray bursts. In 4U 1820 − 30 (top panel) the open triangle shows the observation in which the 'superburst' was discovered (Strohmayer & Brown 2000). Crosses indicate 90 per cent error bars.

2.2.1 *Spectral analysis*

For the spectral analysis we have used PCA Standard2 and HEXTE Standard Mode data. For PCA data reduction we have subtracted the background estimated using PCABCKEST v3.0, produced the detector response matrix with PCARSP v8.0, and analysed the energy spectrum in the range 3–20 keV. For the HEXTE data we have extracted energy spectra (channels 15–61) from cluster A, subtracted the background, corrected for deadtime using the standard FTOOLS v5.2 procedures and analysed the spectra between 20 and 50 keV. A conservative systematic error of 0.75 per cent was added to the PCA data to account for uncertainties in the calibration.

In the case of 4U 1820 − 30, all the 3–50 keV energy spectra obtained simultaneously with radio observations are well fitted with a CompTT model (Titarchuk 1994) corrected for photoelectric absorption (without any need for extra blackbody components: see Bloser et al. 2000); in the worst case we obtain $\chi^2_{\mathrm{re}} = 1.1$ with 49 d.o.f. ($\chi^2_{\mathrm{re}} = \chi^2$/d.o.f.). The equivalent hydrogen column density N_{H} is fixed to 3×10^{21} cm^{-2} (e.g. Bloser et al. 2000). Using this model we obtain (Wien) temperatures kT_0 of the seed photons around 0.6 keV and temperatures of the plasma of about 2.5–3 keV, with a plasma optical depth $\tau \sim 7$.

For Ser X-1, using the same model that successfully fitted the spectra of 4U 1820 − 30, i.e. CompTT corrected for photoelectric absorption (N_{H} was fixed to 5×10^{21} cm^{-2}: e.g. Oosterbroek et al. 2001), we cannot obtain a χ^2_{re} less than 1.8 (50 d.o.f.). The energy spectrum shows an excess between 6 and 7 keV. Therefore we added a Gaussian emission line around 6.5 keV to the model, obtaining a better fit with $\chi^2_{\mathrm{re}} = 0.8$ (47 d.o.f.). The CompTT model fit gives parameter values similar to those found for 4U 1820 − 30 (i.e. $kT_0 \sim 0.7$ keV, temperatures of the plasma of about 2.6 keV and $\tau \sim 6$). In Table 1 we show the unabsorbed 2–10 keV fluxes of Ser X-1 and of 4U 1820 − 30 using the CompTT model (plus a Gaussian emission line in the case of Ser X-1).

2.2.2 *Timing analysis*

For the production of the power spectra we have used EVENT data with a time resolution of 125 μs. We rebinned the data in time to obtain a Nyquist frequency of 4096 Hz. For each observation we created power spectra from segments of 128-s length, using fast Fourier transform techniques (van der Klis 1989 and references therein); we removed detector drop-outs from the data, but no background subtraction was performed. No deadtime corrections were done before creating the power spectra. We averaged the power spectra and subtracted the Poisson noise spectrum applying the method of Zhang et al. (1995), shifted in power to match the spectrum between 3000 and 4000 Hz (see Klein-Wolt, Homan & van der Klis, in preparation). The Leahy normalization was applied (Leahy et al. 1983) and then we converted the power spectra to squared fractional rms. We have fitted the power spectra with a multi-Lorentzian model [e.g. Belloni, Psaltis & van der Klis (2002) and references therein], and plotted in the νP_ν representation (with P_ν the normalized power and ν the frequency). We need two to four Lorentzians to fit the seven power spectra of 4U 1820 − 30: a broad Lorentzian to fit the very low-frequency noise (VLFN), one or two Lorentzians around 10–20 Hz to fit the break of the peaked noise component [$L_{\rm b}$; see van Straaten, van der Klis & Méndez (2003) for details on terminology] and a higher frequency feature ($L_{\rm h}$). In one observation (MJD 52482, see Fig. 2) we also need one narrow Lorentzian to fit a QPO around 100 Hz ($L_{\rm h\,Hz}$). We have fitted the two power spectra of Ser X-1 with four Lorentzians: a broad Lorentzian for the VLFN, one at 15 Hz, one around 30 Hz and, only in one of the two observations (see Fig. 2), a narrow one at ∼70 Hz. The last three features are consistent with being identified either as $L_{\rm b}$, $L_{\rm h}$ and $L_{\rm h\,Hz}$ (as in the 4U 1820 − 30 power spectrum), or as $L_{\rm b2}$, $L_{\rm b}$ and $L_{\rm h}$.

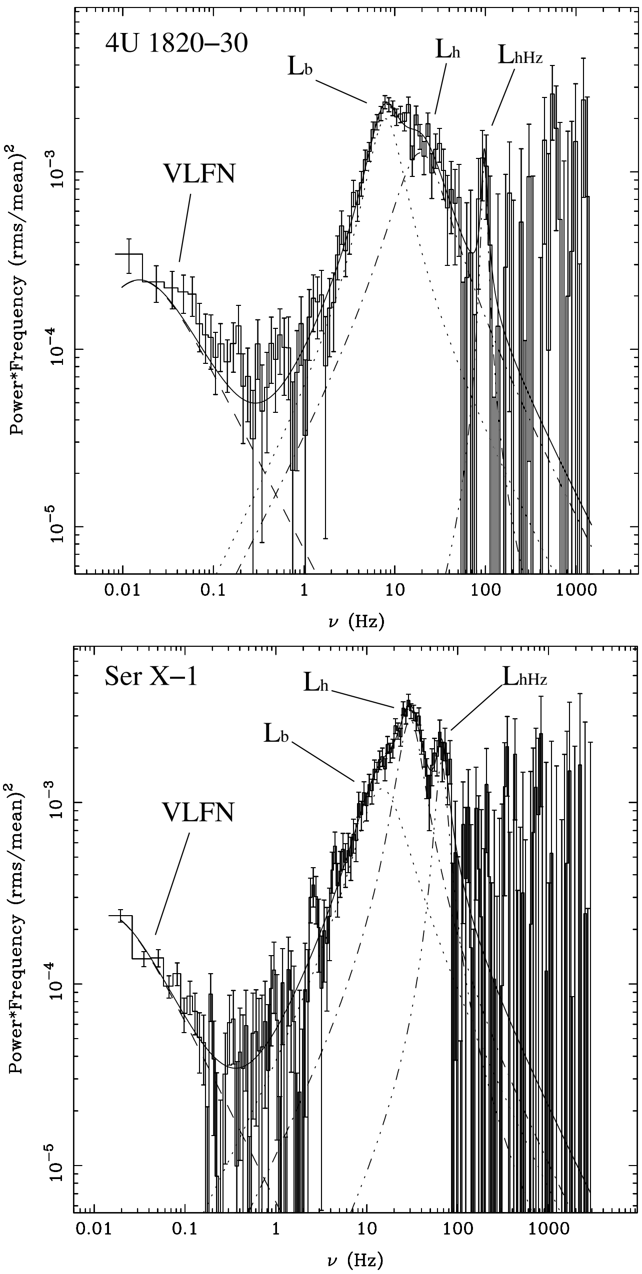

Figure 2. Power spectra of 4U 1820 − 30 on MJD 52482 (top panel) and of the second observation on MJD 52421 of Ser X-1 (bottom panel) with the best-fitting model. Indicated are the four Lorentzian components fitting the VLFN, the break frequency ($L_{\rm b}$), the high-frequency feature ($L_{\rm h}$) and the hecto-Hz QPO ($L_{\rm h\,Hz}$) (but see Section 2.2.2).

3 RESULTS AND DISCUSSION

3.1 4U 1820 − 30

The CD of 4U 1820 − 30 (Fig. 1, top) shows that the simultaneous radio/X-ray observations are in the middle–upper banana. This is consistent with the power spectra characteristics: the presence of VLFN (the integrated fractional rms of the fitting Lorentzian is ∼3 per cent) is typical of atoll sources in a soft X-ray state (i.e. middle–upper banana: see e.g. van Straaten et al. 2002); the absence of kHz QPOs characterizes the power spectra of 4U 1820 − 30 in the middle–upper banana (Zhang et al. 1998; Bloser et al. 2000). The source is detected at 8.46 GHz with a flux density of 0.10 ± 0.02 mJy and marginally detected (∼3σ) at 4.86 GHz with a flux density of 0.13 ± 0.04 mJy in the combined data (see Table 1). The mean (dual-frequency) radio spectrum has a spectral index $\alpha = -0.48 \pm 0.62$ (where $S_\nu \propto \nu^\alpha$ and S_ν is the radio flux density at a frequency ν) consistent with either an optically thin or an optically thick spectrum. Biggs et al. (1994) reported radio detections (at 0.4, 0.6, 1.4 and 1.7 GHz) of a pulsar, PSR 1820 − 30A. The position of this pulsar [see Stappers (1997) for a more accurate timing position] is coincident within 2σ with the optical position of the X-ray binary 4U 1820 − 30 (Sosin & King 1995), and with the position of our radio detection (see Table 2 and Fig. 3). From the positions listed in Table 2 and using a distance to the sources of ∼7 kpc, we infer a lower limit on the physical separation between PSR 1820 − 30A and 4U 1820 − 30 of the order of a few × 10^{16} cm.

In Fig. 3 we directly compare the positions of the sources, plotting the positions listed in Table 2 on the VLA radio map. To do so, we have to take into account errors in the VLA coordinates due to the phase transfer. Therefore we have to increase the error bars when plotting other positions on top of the VLA map: we add (in quadrature) to the non-VLA (i.e. the X-ray binary optical counterpart and the pulsar) positions an additional error of 0.098 arcsec. Moreover, in the case of the PSR 1820 − 30A (timing) position, there is a systematic offset due to the transfer from the timing frame to the VLA frame. Based on Fomalont et al. (1992), we add (in quadrature) an error of 0.005 arcsec in right ascension and 0.02 arcsec in declination to the pulsar position errors. Two other pulsars are identified in NGC 6624: PSR 1820 − 30B (Biggs et al. 1990, 1994), which is too far from the 4U 1820 − 30 optical position to contaminate our radio detection, and PSR 1820 − 30C (Chandler 2002), for which no coordinates are reported. In Fig. 3 we show the VLA radio contour map of 4U 1820 − 30 at 8.46 GHz. The crosses indicate the *Hubble Space Telescope* (*HST*) optical position of the X-ray binary (Sosin & King 1995) and the Parkes radio timing position of the pulsar PSR 1820 − 30A (Stappers 1997).

How do we know whether our radio detection comes from the X-ray binary or from the pulsar PSR 1820 − 30A, since they are positionally coincident? Fig. 4 shows the broad-band (0.4–1.5 GHz) spectrum of the radio source. The dash–dotted line is the best-fitting

Table 2. Positions (with 1σ errors) of the optical and radio counterparts of the X-ray binary 4U 1820 − 30 and the radio (timing) position of the pulsar PSR 1820 − 30A.

	Position	J2000	Errors[a]
VLA source[b]	RA	$18^{h}23^{m}40\overset{s}{.}4820$	$\pm0\overset{s}{.}0088$
	Dec.	$-30°21'40\overset{''}{.}12$	$\pm0\overset{''}{.}16$
4U 1820 − 30 (*HST*)[c]	RA	$18^{h}23^{m}40\overset{s}{.}453$	$\pm0\overset{s}{.}012$
	Dec.	$-30°21'40\overset{''}{.}08$	$\pm0\overset{''}{.}15$
PSR 1820 − 30A[d]	RA	$18^{h}23^{m}40\overset{s}{.}4840$	$\pm0\overset{s}{.}0006$
	Dec.	$-30°21'39\overset{''}{.}96$	$\pm0\overset{''}{.}05$

[a]To compare directly the positions on the VLA map, as we do in Fig. 3, we have to add (in quadrature) an error of 0.098 arcsec to the non-VLA positions, plus an additional error to the pulsar position due to a systematic offset between the timing and the VLA frame (see Section 3.1). [b]Our detection. [c]Sosin & King (1995). [d]Stappers (1997).

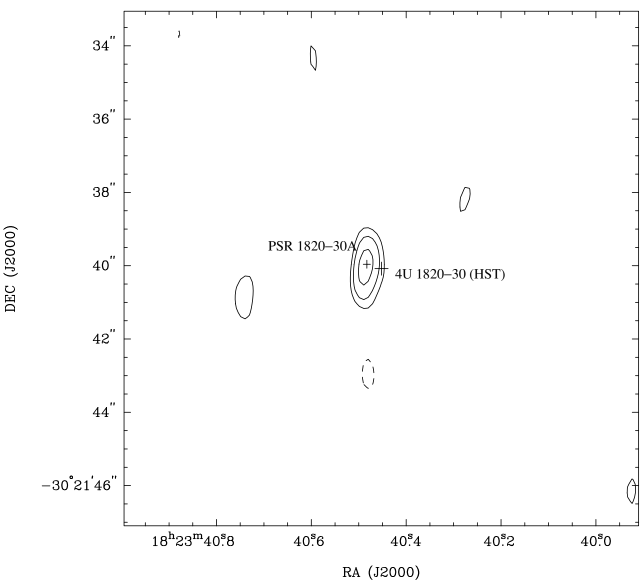

Figure 3. Naturally weighted VLA radio contour plot of the averaged data of 4U 1820 − 30 at 8.46 GHz. We have chosen the contour interval as the rms of the image (0.015 mJy) and plot contours at −4, −2.83, 2.828, 4 and 5.657 times the contour interval. The naturally weighted synthesized beam width is 1.96×0.80 arcsec^2 in position angle $-2\overset{\circ}{.}2$. The crosses indicate the *HST* position of the X-ray binary and the radio timing position of the pulsar PSR 1820 − 30A (see Table 2 and Section 3.1). The sizes of the crosses indicate 1σ errors on the position.

power law of the data from Biggs et al. (1994) and the dashed line is the best-fitting power law of the data from Toscano et al. (1998); both of these fits are for the low-frequency (<2 GHz) radio spectrum and are typical for radio pulsars. The radio spectrum of Toscano et al. (1998, the flatter of the two spectra in Fig. 4) is very steep, with $\alpha \sim -2.9$. The radio flux density at 1.4 GHz is ~0.7 mJy. This spectrum would predict ~4 μJy at 8.5 GHz, 30 times less than we detect (open diamonds in Fig. 4). The spectrum of the pulsar from Biggs et al. (1994), with $\alpha \sim 3.7$, is even more discrepant. The overall spectrum that we observe in Fig. 4 seems to be the superposition of two main spectra, coming from two physically distinct but spatially unresolved sources. We suggest that below ~2 GHz the pulsar dominates the radio emission with a steep spectrum, while the X-ray binary dominates the radio emission above ~2 GHz with a flatter spectrum. Other radio detections above ~1.5 GHz show

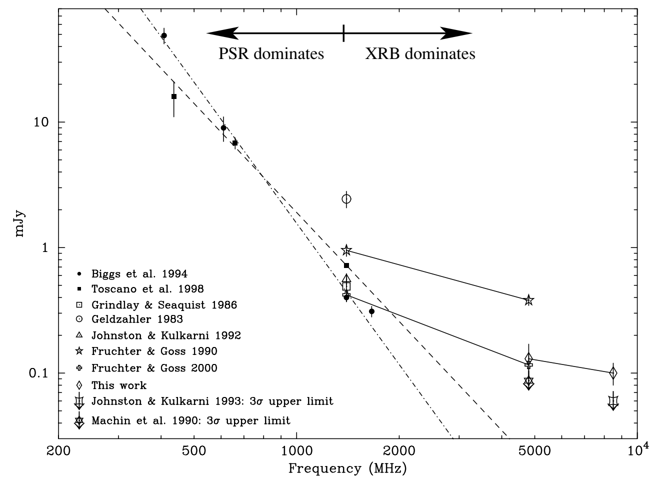

Figure 4. Radio flux density versus frequency of the published radio observations of the pulsar PSR 1820 − 30A and the X-ray binary 4U 1820 − 30. The dashed line is the best-fitting power law of the pulsar observations from (Toscano et al. 1998, black dots) and the dashed-dotted line is the best-fitting power law of the pulsar observations from Biggs et al. (1994, black squares). The solid lines are the power-law fits of the dual-frequency radio observations at 1.5 and 5 GHz (open stars: Fruchter & Goss 1990; open crosses: Fruchter & Goss 2000), and at 5 and 8.5 GHz (open diamonds: this work).

large variability of the flux: at 4.8 GHz the flux density varies from a non-detection with an rms of 0.020 mJy (Johnston & Kulkarni 1993) to a detection of 0.38 ± 0.035 mJy (Fruchter & Goss 1990). Previous dual-frequency radio detections at 1.5 and 5 GHz (Fruchter & Goss 1990, 2000, solid lines in Fig. 4) show flat spectra consistent with the spectrum that we find with our detections at 5 and 8.5 GHz. This further supports the idea that the X-ray binary dominates above ~1.5 GHz and therefore suggests that flux variations in this frequency range are due to 4U 1820 − 30. The possibility that the flattening in the radio spectrum at high frequency is due to emission from a pulsar wind nebula (PWN) seems unlikely. First of all, the source shows a large radio flux variability (more than one order of magnitude at 1.4 GHz; see Fig. 4), unlike PWN. Moreover, a relatively dense interstellar medium (ISM) and/or a high space velocity are required for the pulsar to power a wind nebula. The former condition makes globular clusters, lacking in dense ISM, an unlikely environment in which to find PWN (no PWN in globular clusters are in fact known). In the case of a high space velocity, the pulsar would have already escaped the central region of the cluster by now. The consistency with the Ser X-1 radio detection (e.g. similar radio luminosity at a similar X-ray luminosity and state) further supports our interpretation (see below).

3.2 Ser X-1

The CD of Ser X-1 (Fig. 1, bottom) indicates that the source is in the middle banana X-ray state during the radio observations. This is supported by the variability properties, e.g. the presence of VLFN (rms ~3 per cent), which are typical for an atoll source in its soft state (e.g. van Straaten et al. 2002). In both 4U 1820 − 30 and Ser X-1 we find similar spectral components in the energy spectra, which confirms that the sources are both in a similar (soft) state. We have detected for the first time the radio counterpart of Ser X-1, with a flux density at 8.46 GHz of 0.08 ± 0.02 mJy (see Table 1). This detection is consistent with the previous upper limit of < 0.4 mJy at 5 GHz of Grindlay & Seaquist (1986). Wachter (1997) showed that

Table 3. Optical positions (with 1σ errors) of the DN, DSe and DSw stars (open circles in Fig. 5) and the position (with 1σ errors) of the radio counterpart (cross in Fig. 5) of the X-ray binary Ser X-1.

	Position	J2000	Errors[a]
Ser X-1 (VLA)	RA	$18^{h}39^{m}57^{s}.557$	$\pm0^{s}.010$
	Dec.	$+05^{\circ}02'09''.50$	$\pm0''.14$
DN	RA	$18^{h}39^{m}57^{s}.61$	$\pm0^{s}.02$
	Dec.	$+05^{\circ}02'11''.67$	$\pm0''.36$
DSe	RA	$18^{h}39^{m}57^{s}.56$	$\pm0^{s}.02$
	Dec.	$+05^{\circ}02'09''.74$	$\pm0''.36$
DSw	RA	$18^{h}39^{m}57^{s}.49$	$\pm0^{s}.02$
	Dec.	$+05^{\circ}02'09''.51$	$\pm0''.36$

[a]To compare directly the positions on the optical image, as we do in Fig. 5, we have to add (in quadrature) an error of 0.36 arcsec to the VLA position of Ser X-1 (see Section 3.2).

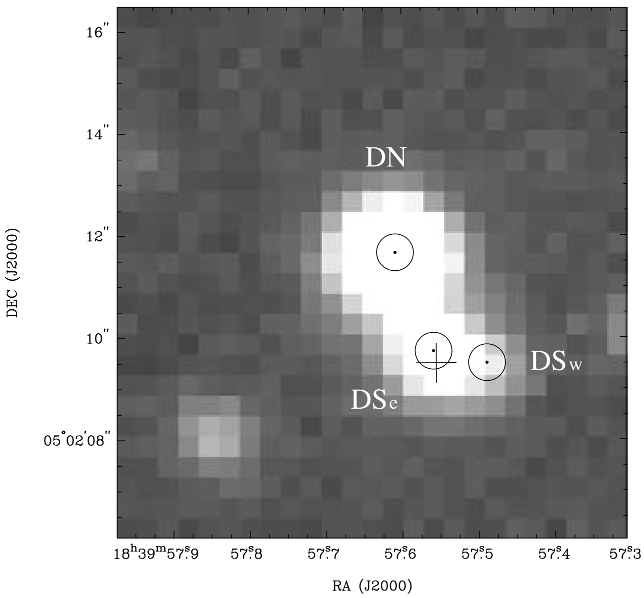

Figure 5. Portion of the optical (*R*-band) image of the field of MM Ser, with the three stars: DN, DSe and DSw (see Wachter 1997). The positions (with 1σ errors) of the three stars are marked with open circles; the position (with 1σ errors) of the radio counterpart is indicated with a cross (see Table 3 and Section 3.2).

MM Ser, the optical counterpart of Ser X-1, is actually the superposition of two stars separated by 1 arcsec. Therefore the position of the radio counterpart allows us to identify the correct optical counterpart. In Fig. 5 we show the optical image of the three stars (DN, DSe and DSw) with positions and errors marked with open circles. The optical image is a 400-s *R*-band exposure obtained with the Cerro Tololo Inter-American Observatory (CTIO) 0.9-m telescope on 1996 July 11 [for details on the reduction and calibration of the image see Wachter (1997)]. An astrometric solution for the 3 × 3 arcmin^2 frame was derived by utilizing 40 stars from the USNO-A2.0 catalogue and the IRAF task CCMAP. The errors on the optical positions are a combination of the uncertainties due to the USNO A-2.0 system (0.3 arcsec) and to the transfer of that coordinate system on to the Ser X-1 frame (0.2 arcsec). The cross indicates our VLA position (with 1σ errors) of the radio counterpart (see Table 3). We clearly see that the radio position is coincident within uncertainties with DSe. From the spectral identification of Hynes et al. (2004) and our positional identification, we can definitely confirm that DSe is MM Ser, the actual optical counterpart of Ser X-1.

3.3 Radio/X-ray correlation in X-ray binaries

The simultaneous radio and X-ray detections of 4U 1820 − 30 and Ser X-1 add new information to the radio/X-ray relations in X-ray binaries. These two atoll sources are both steadily in the soft (banana) state. The radio emission of BHCs in the low/hard state increases as the X-ray flux increases and then decreases drastically (it is ‘quenched’) by a factor of > 50, when the source enters a softer (high/soft or intermediate) X-ray state. In 4U 1728 − 34 in the hard state (mostly island with two excursions to the lower banana), a similar correlation has been observed (Migliari et al. 2003). One data point (the one with the highest X-ray luminosity) lay off the correlation, possibly (even if, oddly, this observation is still in the island state) indicating a radio ‘quenching’. We have now detected the radio counterparts of two NS systems in the soft state (middle–upper banana, with X-ray luminosities higher than those of 4U 1728 − 34) at radio luminosities close to that found in 4U 1728 − 34 for its highest X-ray luminosity observation. However, in the case of these NS systems the reduction in radio luminosities between the brightest hard state and the soft state seems to be only of a factor of ∼10. This indicates that *if* there is a radio ‘quenching’ also in atoll sources, this would be less extreme than in BHCs. Furthermore, if we compare the luminosities that we have observed for these NS sources and the upper limits on the radio luminosities of the BHCs in the soft state (quenching), we note that in BHCs the radio luminosity is lower than in NSs. In fact, we have detected 4U 1820 − 30 and Ser X-1 at 8.5 GHz with radio luminosities of ∼5.0 × 10^{28} erg s^{-1} (using a distance of 7 kpc) and ∼5.8 × 10^{28} erg s^{-1} (using a distance of 8.4 kpc), respectively. The BHC XTE 1550 − 564 when ‘quenched’ has a radio luminosity upper limit of <1.8 × 10^{28} erg s^{-1} [measured at 8.5 GHz and using a distance to the source of 6 kpc (Corbel et al. 2002)] and GX 339-4 has a radio luminosity upper limit of <2.6 × 10^{28} erg s^{-1} [measured at 5 GHz and using a distance of 6 kpc (Fender et al. 1999)]. Therefore NS X-ray binaries in the soft state (when the jet, at least for BHCs, seems to be suppressed) are more luminous in the radio band than black hole X-ray binaries. This is contrary to other X-ray states, in which the BHCs are more radio-loud, and seems to indicate that a ‘residual’ radio emission is present in the NS systems. This difference from BHCs might be related to the presence of a solid surface and/or to the NS magnetic field. Recent theoretical work (e.g. Meier 2001) seems to support the idea that an efficient jet-like outflow production is associated with a geometrically thick accretion disc (i.e. low/hard state in BHCs), while a suppression of the (observable) jet should happen when the disc becomes geometrically thin (i.e. high/soft state in BHCs). Speculating within this picture, assuming the same jet production processes in NS and black hole X-ray binaries (see Fender et al. 2004), a possible explanation might be that the magnetic field of the NS could interact with the accretion disc, which in the softer states should be closer to the compact object, keeping the disc thick enough not to suppress the jet production mechanisms completely.

4 CONCLUSIONS

We have detected two atoll-type NS X-ray binaries, 4U 1820 − 30 and Ser X-1, at radio wavelengths. In particular, we report the following findings.

(i) We argue that we have detected the radio counterpart of 4U 1820 − 30, which can be spectrally distinguished from the positionally coincident radio pulsar PSR 1820 − 30A. The radio emission of the X-ray binary is dominant at higher frequencies, above ∼2 GHz, and shows a flatter spectrum.

(ii) We have detected for the first time the radio counterpart of Ser X-1; this radio detection allows us to identify star DSe as the optical counterpart of Ser X-1.

(iii) Both 4U 1820 − 30 and Ser X-1 are detected at radio wavelengths while steadily in the banana (soft) state. This is different from 4U 1728 − 34 which has been detected at radio wavelengths in the banana state during transient excursions from the island.

(iv) The radio luminosities in the soft state of 4U 1820 − 30 and Ser X-1 are higher than the radio luminosities in the soft state of BHCs (for which the jet is drastically suppressed). If the pattern of the radio flux versus X-ray flux of atoll sources is analogous to BHCs, then radio 'quenching' in the soft state of atoll sources does not seem to be as extreme as in BHCs.

ACKNOWLEDGMENTS

SM and RPF thank Ben Stappers for very useful discussions. The National Radio Astronomy Observatory is a facility of the National Science Foundation operated under cooperative agreement by Associated Universities, Inc.

REFERENCES

Belloni T., Psaltis D., van der Klis M., 2002, ApJ, 572, 392
Berendsen S. G. H., Fender R. P., Kuulkers E., Heise J., van der Klis M., 2000, MNRAS, 318, 599
Biggs J. D., Lyne A. G., Manchester R. N., Ashworth M., 1990, IAU Circ. No. 4988
Biggs J. D., Bailes M., Lyne A. G., Goss W. M., Fruchter A. S., 1994, MNRAS, 267, 125
Bloser P. F., Grindlay J. E., Kaaret P., Zhang W., Smale A. P., Barret D., 2000, ApJ, 542, 1000
Chandler A. M., 2002, PhD thesis, http://resolver.caltech.edu/CaltechETD:etd-01232003-213508
Christian D. J., Swank J. H., 1997, ApJS, 109, 177
Corbel S., Fender R. P., Tzioumis A. K., Nowak M. A., McIntyre V., Durouchoux P., Sood R., 2000, A&A, 359, 251
Corbel S. et al., 2001, ApJ, 554, 43
Corbel S., Nowak M. A., Fender R. P., Tzioumis A. K., Markoff S., 2003, A&A, 400, 1007
Davidsen A. F., 1975, IAU Circ. No. 2824
Dhawan V., Mirabel I. F., Rodríguez L. F., 2000, ApJ, 543, 373
Falcke H., Biermann P. L., 1996, A&A, 308, 321
Fender R. P., 2004, in Lewin W. H. G. van der Klis M., eds, Compact Stellar X-ray Sources, in press (astro-ph/0303339)
Fender R. P., Hendry M. A., 2000, MNRAS, 317, 1
Fender R. P., Kuulkers E., 2001, MNRAS, 324, 923
Fender R. P. et al., 1999, ApJ, 519, L165
Fender R. P., Wu K., Johnston H., Tzioumis A., Jonker P. G., Spencer R., van der Klis M., 2004, Nat, 427, 222
Fomalont E. B., Goss W. M., Lyne A. G., Manchester R. N., Justtanont K., 1992, MNRAS, 258, 497
Fomalont E. B., Geldzahler B. J., Bradshaw C. F., 2001, ApJ, 558, 283
Friedmann H., Byram E., Chubb T., 1967, Sci, 156, 374
Fruchter A. S., Goss W. M., 1990, ApJ, 365, L63
Fruchter A. S., Goss W. M., 2000, ApJ, 536, 865
Gallo E., Fender R. P., Pooley G. G., 2003, MNRAS, 344, 60
Geldzahler B. J., 1983, ApJ, 264, L49
Giacconi R., Murray S., Gursky H., Kellogg E., Schreier E., Matilsky T., Koch D., Tananbaum H., 1974, ApJS, 27, 37
Grindlay J. E., Seaquist E. R., 1986, ApJ, 310, 172
Grindlay J., Gursky H., Schnopper H., Parsignault D. R., Heise J., Brinkman A. C., Schrijver J., 1976, ApJ, 205, L127
Hackwell J. A., Grasdalen G. L., Gehrz R. D., Cominsky L., Lewin W. H. G., van Paradijs J., 1979, ApJ, 233, L115
Hannikainen D. C., Hunstead R. W., Campbell-Wilson D., Sood R. K., 1998, A&A, 337, 460
Hasinger G., van der Klis M., 1989, A&A, 225, 79
Heasley J. N., Janes K. A., Zinn R., Demarque P., Da Costa G. S., Christian C. A., 2000, AJ, 120, 879
Hjellming R. M., Han X. H., 1995, in Lewin W. H. G., van Paradijs J., van den Heuvel E. P. J., eds, X-ray binaries. Cambridge Uuniv. Press, Cambridge, p. 308
Hynes R. I., Charles P. A., van Zyl L., Barnes A., Steeghs D., O'Brien K., Casares J., 2004, MNRAS, 348, 100
Johnston H. M., Kulkarni S. R., 1992, ApJ, 393, L17
Johnston H. M., Kulkarni S. R., 1993, A&A, 280, 523
Kuulkers E., den Hartog P. R., in 't Zand J. J. M., Verbunt F. W. M., Harris W. E., Cocchi M., 2003, A&A, 399, 663
Leahy D. A., Darbro W., Elsner R. F., Weisskopf M. C., Kahn S., Sutherland P. G., Grindlay J. E., 1983, ApJ, 266, 160
Machin G., Lehto H. J., McHardy I. M., Callanan P. J., Charles P. A., 1990, MNRAS, 246, 237
Meier D. L., 2001, ApJ, 548, L9
Migliari S., Fender R. P., Rupen M., Jonker P. G., Klein-Wolt M., Hjellming R. M., van der Klis M., 2003, MNRAS, 342, L67
Monet D. et al., 1998, USNO-A V2.0, A Catalog of Astrometric Standards. US Naval Observatory Flagstaff Station (USNOFS) and Universities Space Research Association (USRA) stationed at USNOFS
Oosterbroek T., Barret D., Guainazzi M., Ford E. C., 2001, A&A, 366, 138
Penninx W., Lewin W. H. G., Zijlstra A. A., Mitsuda K., van Paradijs J., 1988, Nat, 336, 146
Smale A. P., Zhang W., White N. E., 1997, ApJ, 483, L119
Sosin C., King I. R., 1995, AJ, 109, 639
Stappers B. W., 1997, PhD thesis, MSSSO, Australian National University
Strohmayer T. E., Brown E. F., 2002, ApJ, 566, 1045
Swank J. H., Becker R. H., Pravdo S. H., Saba J. R., Serlemitsos P. J., 1976, IAU Circ. No. 2963
Thorstensen J. R., Charles P. A., Bowyer S., 1980, ApJ, 238, 964
Titarchuk L., 1994, ApJ, 276, L41
Toscano M., Bailes M., Manchester R. N., Sandhu J. S., 1998, ApJ, 506, 863
Vacca W. D., Lewin W. H. G., van Paradijs J., 1986, MNRAS, 220, 339
van der Klis M., 1989, ARA&A, 27, 517
van der Klis M., 1994, ApJS, 92, 511
van Straaten S., van der Klis M., Di Salvo T., Belloni T., 2002, ApJ, 568, 912
van Straaten S., van der Klis M., Méndez M., 2003, ApJ, 596, 1155
Wachter S., 1997, ApJ, 490, 401
Zhang W., Jahoda K., Swank J. H., Morgan E. H., Giles A. B., 1995, ApJ, 449, 930
Zhang W., Smale A. P., Strohmayer T. E., Swank J. H., 1998, ApJ, 500, L171

This paper has been typeset from a TEX/LATEX file prepared by the author.